Expanded View Figures

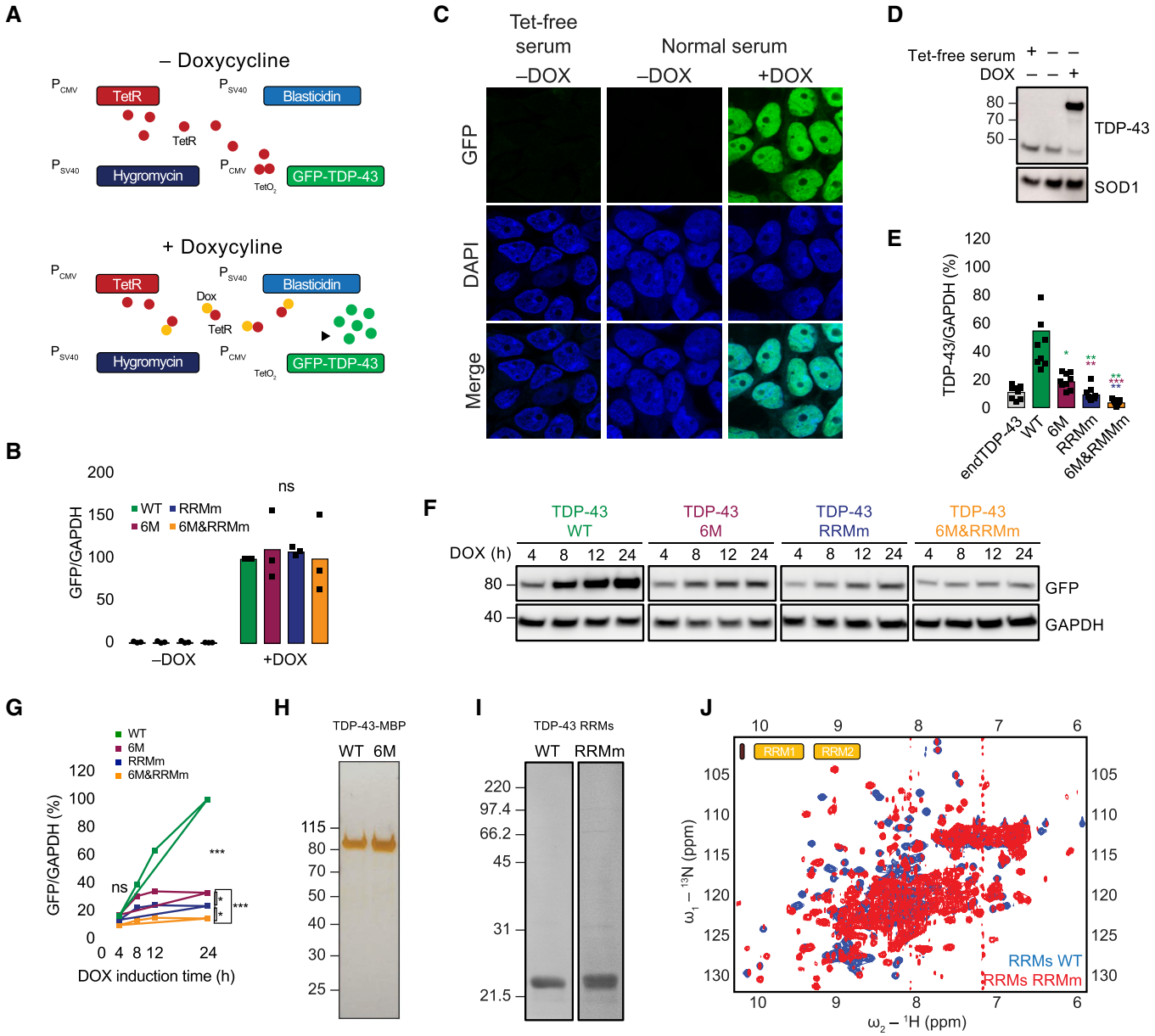

Figure EV1.

Figure EV1. Characterization of the expression levels, localization, and folding of the TDP-43 variants.

A Schematic representation of the Flp-In T-Rex system. Dox: doxycycline, GFP: green fluorescent protein, TetR: tetracycline repressor.

B RNA levels of the GFP-TDP-43 variants after 48 h of expression in the isogenic cell lines measured by qPCR with primers specifically targeted to the GFP sequence. $N = 3$ independent experiments. Two-way ANOVA with Tukey's multiple comparisons *post hoc* test.

C Representative image of confocal fluorescence microscopy showing the tight expression regulation of the Flp-In T-Rex system, which is unaffected by the residual tetracycline (Tet) present in the regular serum used for the preparation of cell culture medium. Expression of GFP-TDP-43 WT is only observable upon addition of doxycycline (DOX) for 48 h. Nuclei are stained with DAPI. Scale bar: 20 μm.

D Western blot analysis of the conditions described in (C).

E Quantification of the TDP-43 signal from Fig 1B using a total TDP-43 antibody, including endogenous TDP-43 (endTDP-43) and the four GFP-TDP-43 variants. $N = 3$ independent experiments. Repeated measures one-way ANOVA with Greenhouse–Geisser correction and Tukey's multiple comparisons *post hoc* test.

F Western blot analysis of a time course of the different GFP-TDP-43 variant expression upon induction with DOX.

G Quantification of the GFP signal from (F). $N = 3$ independent experiments. Two-way ANOVA with Tukey's multiple comparisons *post hoc* test.

H Silver-stained gel showing the purity of 1 μg of the isolated TDP-43-MBP variants. (I) Coommasie stained gel showing the purity of the purified TDP-43 RRM constructs.

I Overlay of 2D ^{1}H-^{15}N HSQC spectra from purified His-tagged, ^{15}N-isotopically labeled TDP-43 RRMs WT (blue) and RRMm RRMs (red). The presence of dispersed peaks in the spectra indicates that both WT and RRMm RRMs are folded, and are compatible with the formation of α-helix and β-strand structures. In case of unfolding, all ^{1}H NMR signals would pool around 8 ppm. ns: not significant, $*P < 0.05$, $**P < 0.01$, $***P < 0.001$. Graph bars represent mean ± SD.

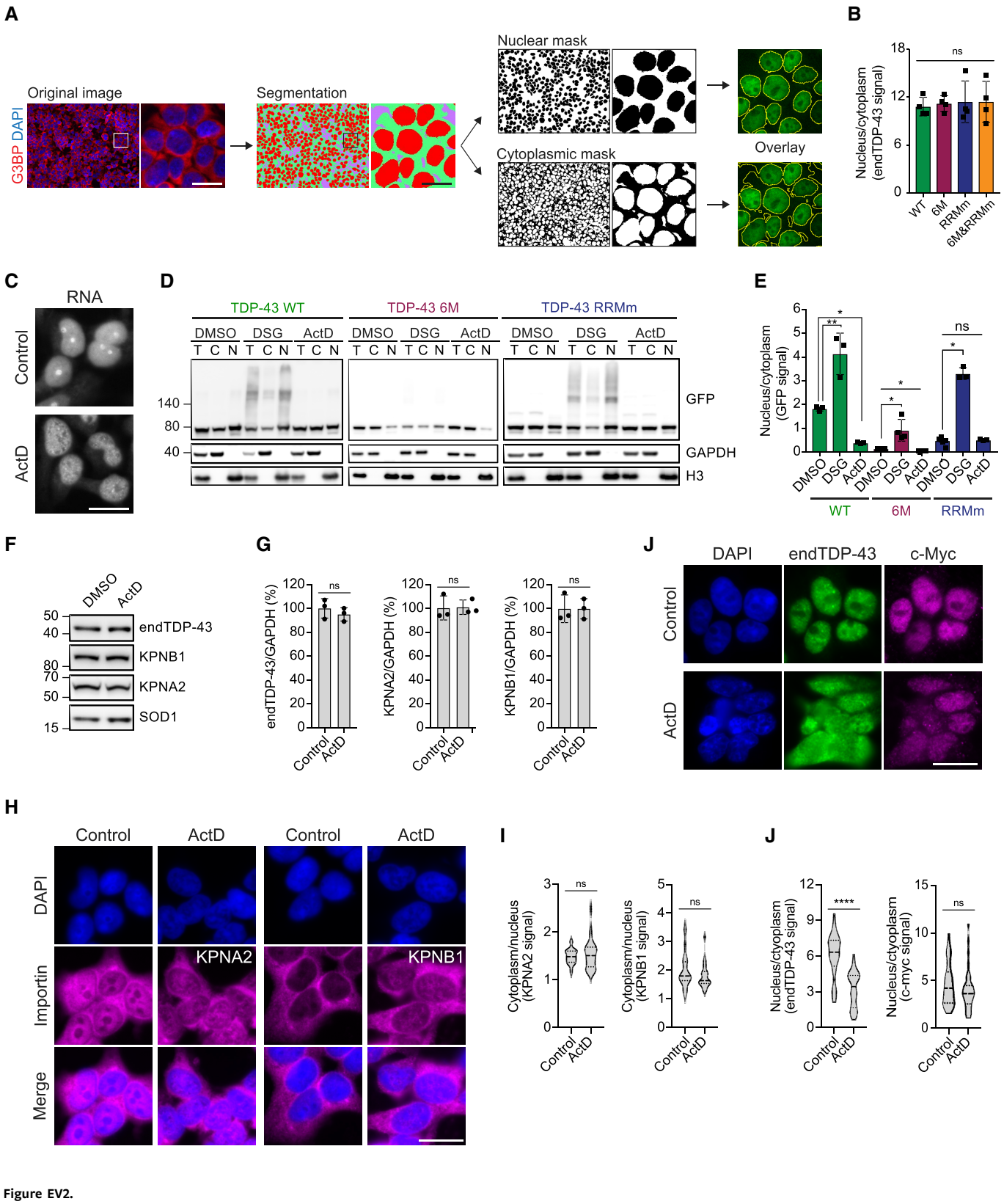

Figure EV2.

Figure EV2. Oligomerization and RNA-binding preserve the nuclear localization of the GFP-TDP-43 variants.

A Schematic of the pipeline for the quantification of nuclear and cytoplasmic GFP-TDP-43 fluorescence levels with the Fiji plug-in Trainable Weka Segmentation. Scale bar: 20 μm.

B Quantification of endogenous TDP-43 (endTDP-43) signal from Fig 2D. $N = 3$ independent experiments. Repeated measures one-way ANOVA with Greenhouse–Geisser correction and Tukey's multiple comparisons *post hoc* test. ns: not significant. Graph bars represent mean ± SD.

C Representative images of widefield fluorescence microscopy of HEK293 cells treated with ActD showing the total RNA pattern. Note the absence of rRNA staining in the nucleoli upon ActD treatment indicating that RNA transcription has been halted. Scale bar: 20 μm.

D After expression of GFP-TDP-43 (WT, 6M or RBDm) for 48 h, the cell lines were treated with 5 μg/ml ActD for 4 h to inhibit transcription or DSG to cross-link protein–protein interactions before performing nucleocytoplasmic fractionation and western blot analysis. Note how the fractionation of the RNA-binding mutant GFP-TDP-43 (RRMm) resembles that of ActD-treated GFP-TDP-43 WT, and how the stabilization of TDP-43 oligomerization through DSG cross-link does not affect the localization of oligomerization-deficient GFP-TDP-43 as much as it does for the oligomerization-competent GFP-TDP-43 WT.

E Quantification of the GFP signal from (D). $N = 3$ independent experiments. Repeated measures one-way ANOVA with Tukey's multiple comparisons *post hoc* test.

F Expression of the importins involved in the nuclear translocation of TDP-43 (KPNA2 and KPNB1) was analyzed in HEK293 cells by western blot upon treatment with 5 μg/ml ActD for 4 h.

G Quantification of the endogenous TDP-43 (endTDP-43), KPNA2, and KPNB1 signal from (E). Repeated measures one-way ANOVA with Greenhouse–Geisser correction and Dunnett's multiple comparisons *post hoc* test. (H) Representative images of widefield fluorescence microscopy of HEK293 cells treated with 5 5 μg/ml ActD for 4 h showing the distribution of KPNA2 and KPNB1. Scale bar: 20 μm.

H Quantification of the nucleocytoplasmic distribution of KPNA2 and KPNB1 in the immunocytochemistry images shown in (H). $N = 25$ cells. Unpaired two-tailed *t*-test.

I Representative images of widefield fluorescence microscopy of HEK293 cells treated with 5 μg/ml ActD for 4 h showing the distribution of c-myc, a non-RNA-binding cargo of the KPNA2/KPNB1 complex. Scale bar: 20 μm.

J Quantification of the endogenous TDP-43 (endTDP-43) and c-myc levels in the immunocytochemistry images shown in (I). $N = 40$ cells. Mann–Whitney *U*-test. Nuclei are stained with DAPI in (A, H and J). Ns: not significant, $*P < 0.05$, $**P < 0.01$, $****P < 0.0001$. Graph bars represent mean ± SD. Violin plots show mean and quartiles.

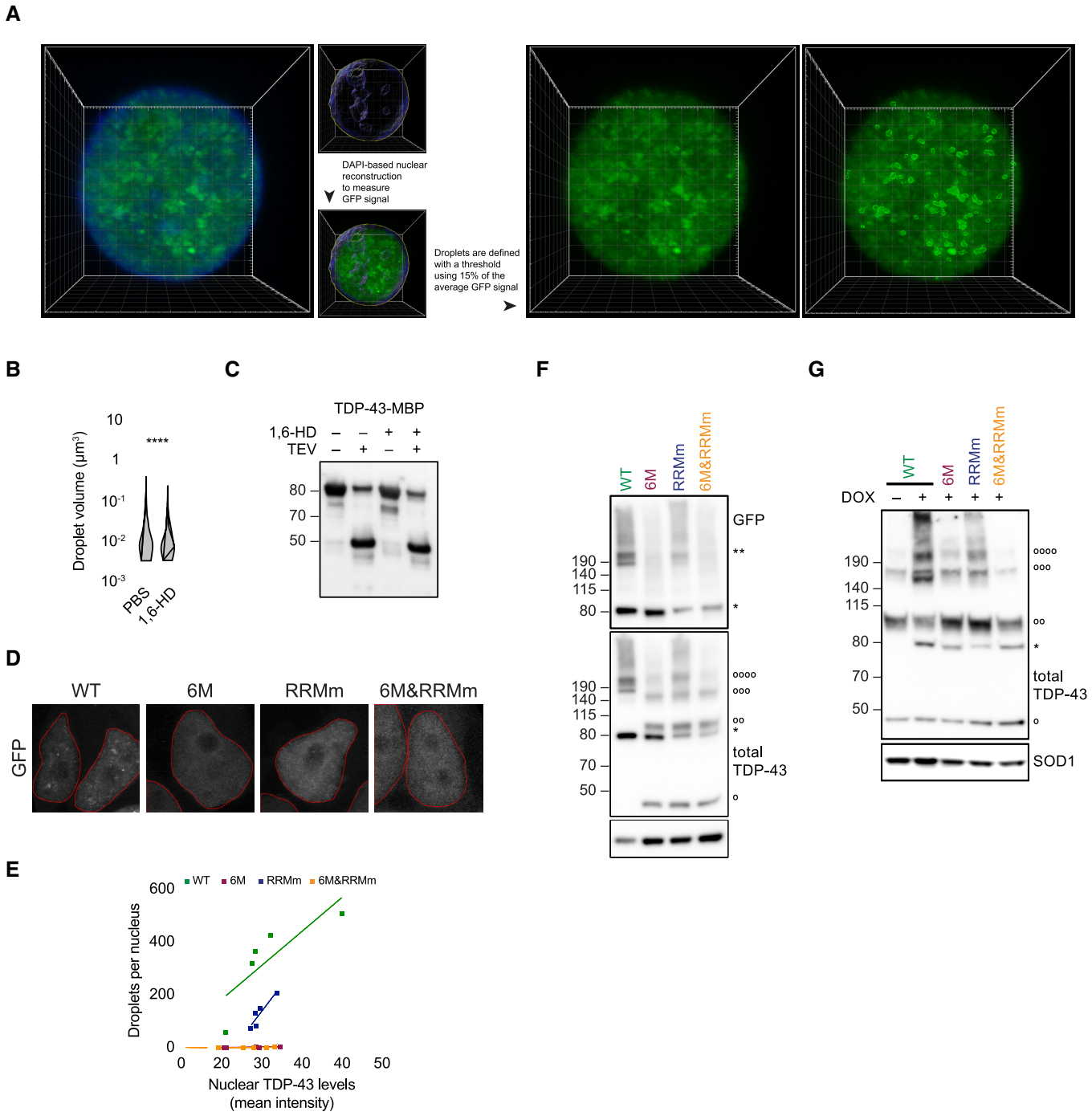

Figure EV3.

Figure EV3. Oligomerization retains TDP-43 in the nucleus in both RNA-bound and -unbound states.

A Schematic of the Imaris pipeline for the quantification of the average nuclear TDP-43 fluorescence as well as the definition of the nuclear TDP-43 droplets that were subsequently analyzed for total number and volume. Pipeline shown for GFP-TDP-43 signal, but the same approach was used with fluorescence derived from the immunostaining of endogenous TDP-43.

B 3D quantification of the volume of the nuclear droplets per cell in the conditions described in Fig 3A. $N = 344–1,679$ droplets. Mann–Whitney *U*-test.

C Western blot analysis of the cleavage of the maltose-binding protein (MBP) tag of recombinant full-length TDP-43 by TEV protease for the *in vitro* LLPS assay shown in Fig 2C. Note that the presence of 1,6-hexanediol (1,6-HD) does not affect the cleavage of the tag.

D Representative maximum intensity Z-projections (thickness of ~ 10 μm, in steps of 0.21 μm) from confocal fluorescence microscopy of the isogenic cell lines expressing GFP-TDP-43 for 4 h with doxycycline (DOX). Scale bar: 5 μm.

E 3D quantification of the number of nuclear droplets per cell after GFP-TDP-43 expression for 4 h. $N = 5$ cells.

F Expression of GFP-TDP-43 variants was induced for 48 h before DSG cross-linking of protein–protein interactions and subsequent analysis by western blot. * and ** indicate GFP-TDP-43 monomers and dimers, respectively. °, °°, °°°, and °°°° indicate endogenous TDP-43 (endTDP-43) monomers, dimers, trimers, and tetramers.

G Expression of GFP-TDP-43 variants was induced for 4 h before DSG cross-linking of protein–protein interactions and subsequent analysis by western blot. * indicates GFP-TDP-43 monomers. °, °°, °°°, and °°°° indicate endTDP-43 monomers, dimers, trimers and tetramers. $^{**}P < 0.01$, $^{****}P < 0.0001$. Violin plots show mean and quartiles.

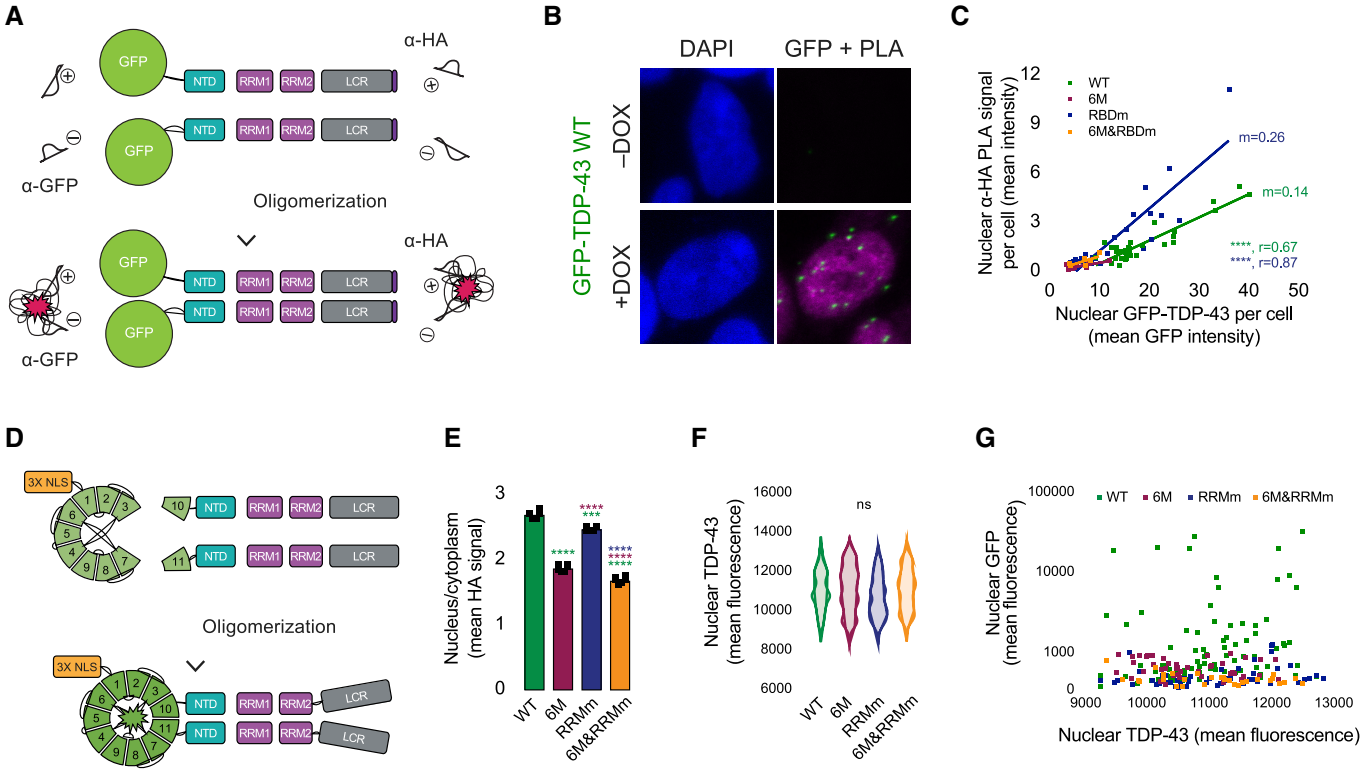

Figure EV4. Nuclear TDP-43 oligomers present different features depending on their RNA binding state.

A Schematic representation of the proximity ligation assay (PLA) to detect homodimers using a single monoclonal antibody conjugated to two different nucleic acid probes, for both tags at the N-terminus (GFP) or C-terminus (HA) of the GFP-TDP-43 construct.

B PLA using a monoclonal anti-GFP antibody specifically identifies the presence of GFP-TDP-43 WT dimers in the isogenic cell lines upon protein expression with doxycycline (DOX) for 48 h. Note the absence of dimer signal in the absence of GFP-TDP-43 expression (–DOX). Nuclei are stained with DAPI. Scale bar: 5 μm.

C Quantification of the nuclear PLA signal obtained using an anti-HA monoclonal antibody in relation to the protein expression levels of the different TDP-43 variants, measured as the mean HA signal. $N = 9–16$ cells.

D Schematic representation of the GFP trimolecular fluorescence complementation (triFC) assay designed to identify TDP-43 dimers. NLS: nuclear localization signal.

E Quantification of nucleocytoplasmic levels of TDP-43 in immunocytochemistry images as shown in Fig 4H. $N = 6$ independent experiments. One-way ANOVA with Tukey's multiple comparisons *post hoc* test.

F Quantification of the average nuclear mean T_{10}- and T_{11}-TDP-43 signals from Fig 4H shows that cells analyzed for reconstituted GFP present comparable protein expression levels of the TDP-43 variants. $N = 30–83$. Kruskal–Wallis test with Dunn's multiple comparisons *post hoc* test.

G Quantification of the nuclear mean GFP fluorescence in relation to the average nuclear mean T_{10}- and T_{11}-TDP-43 signals from Fig 4H indicated that reconstitution of GFP fluorescence is not due to different protein expression levels of the TDP-43 variants. $N = 30–83$. ns: not significant, $^{***}P < 0.001$, $^{****}P < 0.0001$. Graph bars represent mean ± SD.

Figure EV5. Nuclear TDP-43 droplets do not localize to nuclear speckles.

A Representative confocal microscopy images of HEK293 cells stained for the Cajal body marker coilin. Scale bar: 10 μm (5 μm for insets).

B Representative confocal microscopy images of HEK293 cells hybridized with a fluorescent *NEAT1* probe to mark the paraspeckles. The field overview is shown as a maximum intensity Z-projection (thickness of ~ 10 μm, in steps of 0.21 μm). Scale bar: 10 μm (5 μm for insets).

C Representative confocal microscopy images of the isogenic HEK293 lines expressing the different GFP-TDP-43 variants for 24 h and stained for the nuclear speckle marker pSC35.

D 3D analysis quantification showing the percentage of each of the analyzed subnuclear compartments that colocalize with each of the GFP-TDP-43 variants as shown in Fig 5E and F; Appendix Fig S5C. $N = 8$–21 cells. Kruskal–Wallis test with Dunn's multiple comparisons *post hoc* test.

E Representative confocal microscopy images of the isogenic HEK293 lines expressing the different GFP-TDP-43 variants for only 4 h to achieve similar expression levels and stained for the Cajal body marker coilin.

F 3D analysis quantification showing the percentage of Cajal bodies that colocalize with each of the GFP-TDP-43 variants as shown in (E). $N = 39$–54 cells. Kruskal-Wallis test with Dunn's multiple comparisons *post hoc* test. ns: not significant, $^{**}P < 0.01$, $^{****}P < 0.0001$. Violin plots show mean and quartiles.

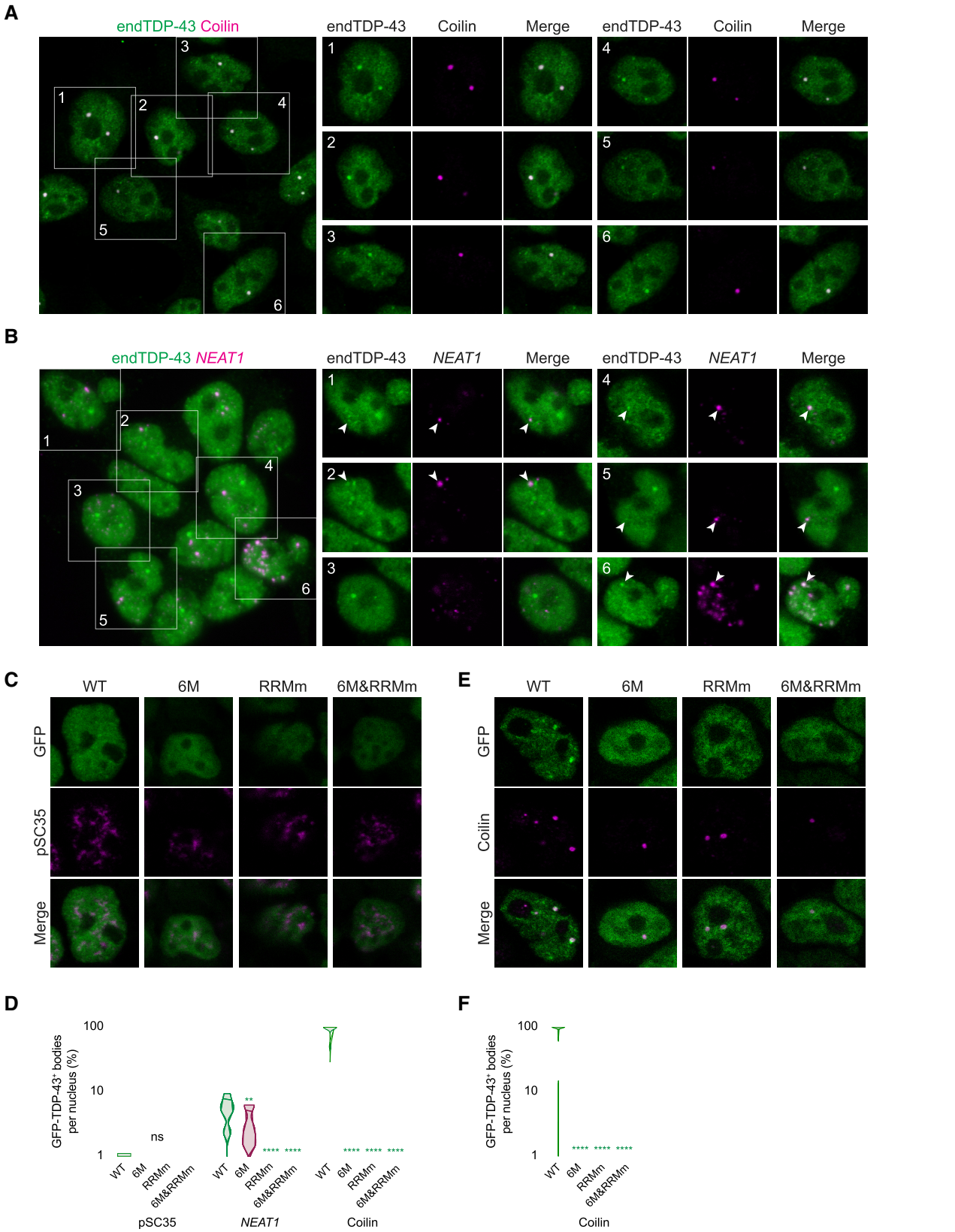
A
endTDP-43 Coilin
endTDP-43
Coilin
Merge
B
endTDP-43 NEAT1
endTDP-43
NEAT1
Merge
C
WT
6M
RRMm
6M&RRMm
GFP
pSC35
Merge
E
WT
6M
RRMm
6M&RRMm
GFP
Coilin
Merge
D
GFP-TDP-43+ bodies per nucleus (%)
100
10
1
ns
**
****
pSC35
NEAT1
Coilin
F
GFP-TDP-43+ bodies per nucleus (%)
100
10
1
****
Coilin

Figure EV5.